Numerical Study of Separated Laminar Boundary Layers over Multiple Sine-Wave Protuberances

A. Polak,* M.J. Werle,† V.N. Vatsa,‡ and S.D. Bertke‡
University of Cincinnati, Cincinnati, Ohio

Supersonic laminar flow over wave-shaped walls with multiple separation bubbles were studied using an implicit finite-difference technique to solve the interacting boundary-layer equations. Solutions for Mach numbers 3 and 6, Reynolds numbers 1×10^5 and 2×10^5, wall temperature to stagnation temperature ratios of 0.45 and 0.675, and the protuberance height to width ratio range of 0 to 0.1 are presented in terms of skin friction and heat transfer distributions for several different protuberance configurations. These numerical results show that after separation occurs the maximum wall shear and heating rates do not increase with protuberance height.

Nomenclature

c_f = normalized skin friction coefficient
c_p = constant pressure specific heat
F = normalized longitudinal velocity, $F=u/u_e$
g = normalized total enthalpy, $g=H/H_e$
h = nondimensional protuberance height
H = nondimensional total enthalpy, $H=H^*/u^{*2}_{\infty}$
ℓ = viscosity parameter, $\ell=\rho\mu/\rho_e\mu_e$
L^* = reference length
M = Mach number
n = nondimensional distance normal to surface, $n=n^*/L^*$
p = nondimensional static pressure, $p=p^*/\rho^*_{\infty}u^{*2}_{\infty}$
P_r = Prandtl number
Q_w = normalized heat transfer coefficient
Re_{∞} = Reynolds number based on freestream viscosity, $Re_{\infty}=\rho^*_{\infty}u^*_{\infty}L^*/\mu^*_{\infty}$
Re_r = Reynolds number based on reference viscosity, $Re_r=Re_{\infty}\mu^*_{\infty}/\mu^*_r(u^{*2}/c_p)$
s = nondimensional distance measured along the surface, $s=s^*/L^*$
t = time
T = nondimensional static temperature, $T=c_pT^*/u^{*2}_{\infty}$
u = viscous nondimensional longitudinal velocity, $u=u^*/u^*_{\infty}$
v = transformed viscous normal velocity
w = nondimensional width of the protuberance
x,y = nondimensional Cartesian coordinates, $x=x^*/L^*$, $y=y^*/L^*$
α = u_e^2/T_e
β = pressure gradient parameters, $(2\xi/u_e)(du_e/d\xi)$
γ = ratio of specific heats
δ = nondimensional displacement thickness
δ_{fp} = flat plate displacement thickness measured at protuberance maximum heating location
ϵ = $1/(Re_r)^{1/2}$
η = transformed normal coordinate
θ_T = angle of deflection of inviscid streamlines
θ_s = slope of surface
μ = nondimensional viscosity, $\mu=\mu^*/\mu^*_r(u^{*2}/c_p)$
ξ = transformed longitudinal coordinate
ρ = nondimensional density, $\rho=\rho^*/\rho^*_{\infty}$

Subscripts

e = inviscid edge values
∞ = freestream values
0 = freestream stagnation value
r = reference values
w = wall values
fp = corresponding flat plate value

Superscript

$*$ = dimensional quantities

Received May 15, 1975; revision received September 4, 1975. The incentive to study this problem came from R.T. Davis to whom the authors express their gratitude. The authors acknowledge with thanks W.C. Volz of the U.S. Naval Air Systems Commands for his continued support during this effort. This work was supported by the U.S. Naval Ordnance Laboratory through contract N 60921-74-C-0203.

Index categories: Boundary Layers and Convective Heat Transfer – Laminar; Jets, Wakes, and Viscid-Inviscid Flow Interactions.

*Associate Professor, Department of Aerospace Engineering. Associate Fellow AIAA.

†Professor, Department of Aerospace Engineering. Associate Member AIAA.

‡Graduate Research Assistant, Department of Aerospace Engineering.

Introduction

In the past decade many theoretical studies have been conducted in the area of separated flows and a high degree of accuracy has been achieved in predicting detailed laminar two-dimensional separation characteristics. Among the various techniques used, the numerical finite-difference method seems to be one of the most efficient, accurate and theoretically sound. Most of these studies[1-3] considered a boundary layer approaching along a flat plate and its subsequent separation induced by a single element (either an impinging shock wave or a compression ramp). Modeling the two-dimensional separation over a protuberance or a set of protuberances placed in tandem involves two or more separation bubbles and until the present study no predictions of such complex flowfields have been attempted.

The objective of the present study was to solve the supersonic interacting laminar boundary-layer equations for flows over a single protuberance or a train of protuberances with multiple separation bubbles by the application of the finite difference numerical algorithm developed recently.[4] A more detailed account about the present study is given in Ref. 5.

Governing Equations

It is assumed here that the interacting boundary-layer equations are sufficient to describe the problem under study.[6] The classical boundary-layer equations are written here in terms of the Levy-Lees transformed coordinates

$$\xi=\int_0^s \rho_e\mu_e u_e ds; \quad \text{and} \quad \eta=\frac{(Re_r)^{1/2}u_e}{(2\xi)^{1/2}}\int_0^n \rho dn \tag{1}$$

New dependent variables are defined as

$$F=u/u_e; \quad g=H/H_e \tag{2}$$

F and g are the normalized s-component of velocity and total enthalpy respectively. The transformed governing equations then are

continuity equation

$$V_\eta + F + 2\xi F_\xi = 0 \tag{3}$$

monentum equation

$$(\ell F_\eta)_\eta - VF_\eta + (1+\alpha/2)\beta\ (g-F^2) - 2\xi FF_\xi = 0 \tag{4}$$

energy equation

$$(\ell g_\eta)_\eta - P_r V g_\eta + (2\alpha/2+\alpha)(P_r - 1)(\ell F F_\eta)_\eta - 2\xi P_r F g_\xi = 0 \tag{5}$$

where V is the transformed normal velocity function and

$$\ell = \rho\mu/\rho_e\mu_e; \quad \text{and} \quad \alpha = u_e^2/T_e, \quad \beta = \frac{2\xi}{u_e}\frac{du_e}{d\xi} \tag{6}$$

and the Prandtl number P_r is taken here as 0.72. The auxiliary relations used are the equation of state for a perfect gas and Sutherland's viscosity law. The governing equations are subject to boundary conditions

$$F(\xi,0) = V(\xi,0) = 0; \quad g(\xi,0) = T_w/T_e;$$
$$F(\xi,\infty) = g(\xi,\infty) = 1 \tag{7}$$

The interaction of the boundary layer with the isentropic supersonic inviscid flow is modeled via the pressure gradient parameter β by coupling it to the inclination θ_T of the total displacement body (see Fig. 1). Namely, the edge pressure is given by the Prandtl-Meyer relation approximated here to second order in terms of θ_T as

$$p_e = \frac{1}{\gamma M_\infty^2} + \frac{\theta_T}{(M_\infty^2-1)^{1/2}} + \frac{(M_\infty^2-2)^2+\gamma M_\infty^4}{4(M_\infty^2-1)^2}\theta_T^2 \tag{8}$$

where

$$\theta_T = \tan^{-1}(d\Delta_T/dx); \quad \Delta_T = y_s + \delta\cos\theta_s \tag{9}$$

$$\delta = \int_0^\infty \left(1 - \frac{\rho u}{\rho_e u_e}\right)dn = \frac{(2\xi)^{1/2}}{(Re_r)^{1/2}\rho_e u_e}$$
$$\int_0^\infty \left(\frac{H_e}{T_e}g - \frac{u_e^2}{2T_e}F^2 - F\right)d\eta \tag{10}$$

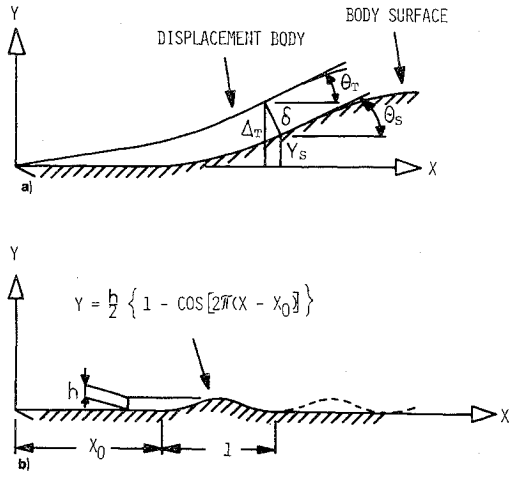

Fig. 1 a) Interaction model; b) surface geometry.

Isentropic relations are used to relate the edge quantitites. The approximation given by Eq. (8) is more appropriate for the present application than the pressure law from the linearized theory[4] because of the higher local flow deflections.

Solution Method

An essential difference between the classical boundary-layer theory and the interacting boundary-layer approach is the appearance of nonunique branching solutions, as was formally shown by Nieland[7] and further studied by Werle, Hankey, and Dwoyer.[8] It is now clear that branching results because of attempts to solve a boundary value problem with initial value techniques.[9] This branching causes some dilemma in recovering the particular solution sought. A shooting technique was developed earlier[2,6] to handle this problem. Recently, Werle and Vatsa[4] developed a new technique which eliminates the awkward search for a solution by the shooting technique. They introduce the downstream compatibility condition that specifies the asymptotic approach of the surface pressure to the inviscid downstream pressure level.

The numerical algorithm applied to the present problem was adopted from Ref. 4. This numerical scheme is first-order accurate in the longitudinal step size. This new alternating-direction-implicit (ADI) method for solving supersonic interacting boundary-layer equations is based on the aforementioned argument that the interacting boundary-layer equations are of the boundary value type rather than the initial value type usually associated with classical parabolic boundary-layer equations. Therefore, a downstream boundary condition must be prescribed to proper formulate the problem. Using a model equation in lieu of the interacting boundary-layer momentum equation, Werle and Vatsa, following the lead of Garvine,[9] showed that due to the interaction, branching solutions exist. These solutions are exponential in character and therefore difficult to control in a marching type numerical procedure, i.e., shooting technique. It was concluded[4] that a relaxation technique employed for solution of elliptic partial differential equations and which allowed incorporation of the downstream boundary condition was applicable here. This was accomplished by introducing an artificial time-like term $\partial\Delta_T/\partial t$ into the momentum equation and then through the use of the ADI relaxation method the sought after steady-state solution is obtained.

The numerical search for the solution proceeds in two time-like half steps which are repeated as many times as needed to obtain a relaxed solution. In present calculations it took 15-20 sweeps to obtain a well converged solution. In the present calculations the solution was considered well settled in time when in the last two consecutive time steps the variation in C_f at any station s appeared only in the third or higher decimal place. Details about the formulation of the numerical algorithm can be found in Ref. 4.

At the initial station ξ_i the calculation starts by assuming the equations to be self-similar. This corresponds approximately to a weakly interacting solution at that station. The deviation from the true solution should be small if this station is sufficiently ahead of the junction of the flat-plate and the protuberance.

An important feature of this new ADI method is that the equations can be solved exactly in the reversed flow region, where forward rather than backward differencing in ξ direction is recommended for numerical stability purposes. This procedure is known as upwind differencing. This can now (in principle) be accomplished by using the downstream information from the previous time step. Because of small velocity component and its streamwise gradient in the reverse flow region, the results obtained from this consistent treatment do not differ appreciably from the previously used approximation in the shooting technique[2,6] where the convective terms were shut out or replaced by a multiple of its negative value where $u \leq 0$. For simplicity we have therefore adopted

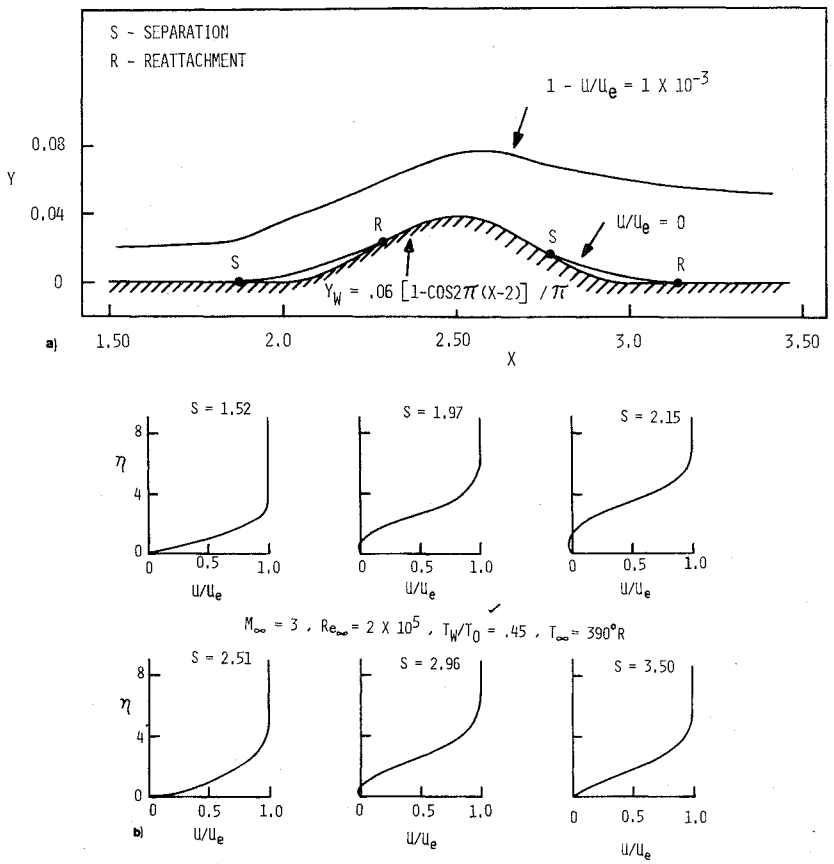

Fig. 2 a) Separated boundary layer over a single protuberance; b) velocity profile evolution.

this approximation in the present calculations recommended originally by Reyher and Flugge-Lotz.[2]

After quasilinearizing the governing equations, the partial derivatives are replaced by finite differences. Central differences were used to represent partials with respect to η, as well as for $d^2\Delta_T/ds^2$ and for $d\Delta_T/ds$ in both sweeps. Backward differences were used for the first partials in ξ and t. The resulting finite-differencing equations were solved by iterative techniques.[5,6]

Results and Discussion

No theoretical studies of interacting boundary layers with multiple separation regions have been made in the past although solutions for attached boundary-layer flow over a wave shaped wall by an inverse method were obtained before by Fannelop and Flugge-Lotz[10] using the implicit finite-difference procedure of Blottner and Flugge-Lotz.[11]

The body geometry considered in the present study consisted of a single or multiple sine-wave protuberances placed on a flat plate (see Fig. 1) with the contoured body profile expressed as

$$y=\frac{h}{2}\left\{1-\cos\left[\frac{2\pi}{w}(x-x_0)\right]\right\}$$

$$\text{for}\quad x_0\le x\le x_0+nw \tag{11}$$

where x_0 was the upstream junction between the flat plate and sine-wave profile, taken to be equal to 2.0 in all but one case here, n was the number of waves, and w was the width of the wave (taken to be unity except for the one case where comparison with experimental data was made; here $w=1.5$). The amplitude $h/2$ of the waves was varied between $0.03/2\pi$-$0.15/2\pi$. Correspondingly, the values of δ_{fp}/h varied between 0.25-1.0 for separated boundary layers.

Although a variety of flow conditions were studied here, a base case was identified for extensive parametric studies. The flow conditions for this study are given as (referred to later as standard values) $M_\infty=3$, $Re_\infty=2\times10^5$, $T_w/T_0=0.45$, $T_\infty=390°R$. Use was made of the Sutherland's viscosity law for air, a Prandtl number of $Pr=0.72$, a specific heat at constant pressure of $C_p=6606\text{ft}^2/\text{sec}^2\,°\text{R}$, a ratio of specific heats of $\gamma=1.4$, and a gas constant $R=1{,}716\text{ ft}^2/\text{sec}^2\,°R$.

For the standard flow values the calculations were initialized with a self-similar solution at $x=0.5$. The step size Δs, along the body contour, was taken 0.03 with 160-200 grid points in the streamwise direction. A grid size refinement study was not performed here but earlier studies[4,6] indicate that $\Delta s=0.03$ is a reasonable step size. The transverse step size $\Delta\eta$ was taken as 0.1 or 0.2 (for higher wall temperature, higher Mach number) with 76 or 101 grid points. Depending on the number of grid points, on the flow parameters, amplitude and number of waves, the computing time on the IBM 370/165 ranged from 15-35 min.

Results of the numerical calculations are given here in terms of normalized skin friction coefficient C_f, normalized surface heat transfer rate Q_w, and displacement thickness parameter δ defined as

$$C_f=\mu_w^*\left(\frac{\partial u^*}{\partial y^*}\right)_w\Big/\frac{\epsilon}{2}\rho_\infty^* u_\infty^{*2}=\frac{2\rho_w\mu_w u_e^2}{(2\xi)^{1/2}}\left(\frac{\partial F}{\partial\eta}\right)_w \tag{12}$$

$$Q_w=\left(k^*\frac{\partial T^*}{\partial y^*}\right)_w\Big/\epsilon\rho_\infty^* u_\infty^{*3}=(1+\alpha/2)\frac{\mu_e\rho_e u_e T_e\ell_w}{Pr(2\xi)^{1/2}}\left(\frac{\partial g}{\partial\eta}\right)_w \tag{13}$$

The distortion of the original flat-plate boundary layer due to the presence of a single sine-wave protuberance with $h=0.12/\pi$ and standard values for the flow parameters is shown in Fig. 2a. The edge of the boundary, defined here as the line $u/u_e=0.999$, and the zero velocity line aid in understanding

the extent of the upstream influence zone, and the downstream recovery zone with two recirculating regions. The corresponding velocity profiles at various stations are shown in Fig. 2b. Notice that the Blasius profile at $x=1.52$ remains distorted at $x=3.50$, that is, a half a wavelength downstream of the protuberance (the protuberance only extends from $x=2$ to $x=3$).

The effect of wave amplitude on the separation characteristics is shown in Fig. 3a, b. For the small bump with height $h=0.06/\pi$ the flow remains attached, for $h=0.09/\pi$ incipient separation occurs, and for $h=0.12/\pi$ very distinctive separation bubbles appear. From the present solutions it was observed that the peak surface heating and the maximum skin friction increase almost linearly for $0<h<0.06/\pi$. Increase in the protuberance height from $h=0.6/\pi$ is still accompanied by increase of the maximum in skin friction and surface heating, but further increase from $h=0.09/\pi$ to $0.12/\pi$, after incipient separation has occurred, causes a slight increase or no increase in maximum of C_f and Q_w.

The effect of the number of waves is shown in Fig. 4 and 5 for $h=0.06/\pi$ and standard flow conditions. At these conditions, no separation occurs over the single wave (Fig. 3a). The skin friction and heat transfer dip near the forward and rear junctions with maxima in the neighborhood of the crest of the wave and a very slow downstream recovery to the flat plate values. Adding a second wave of the same amplitude and wavelength behind the first wave is seen to induce separation between the two waves (Fig. 4, curve 1). The effect of the wake of one protuberance on the separation characteristics of the second one is also shown in Fig. 4, curve 2. Shifting the protuberance downstream from the first one eliminates separation.

When additional waves, one ahead of the first one and one behind the second one are added, two more separation bubbles appear with the middle one increasing in extent. It is to be noted that the drop in skin friction and heating rates maxima is faster than the drop of the corresponding flat plate levels. (Fig. 5a,b).

Figure 5c shows some interesting features of the disturbed flow field caused by a train of sine-waves for the flow conditions given in Figs. 5a,b. Over the first wave, where the boundary-layer is still attached, the pressure variation resembles a sinusoidal curve and the averaged displacement

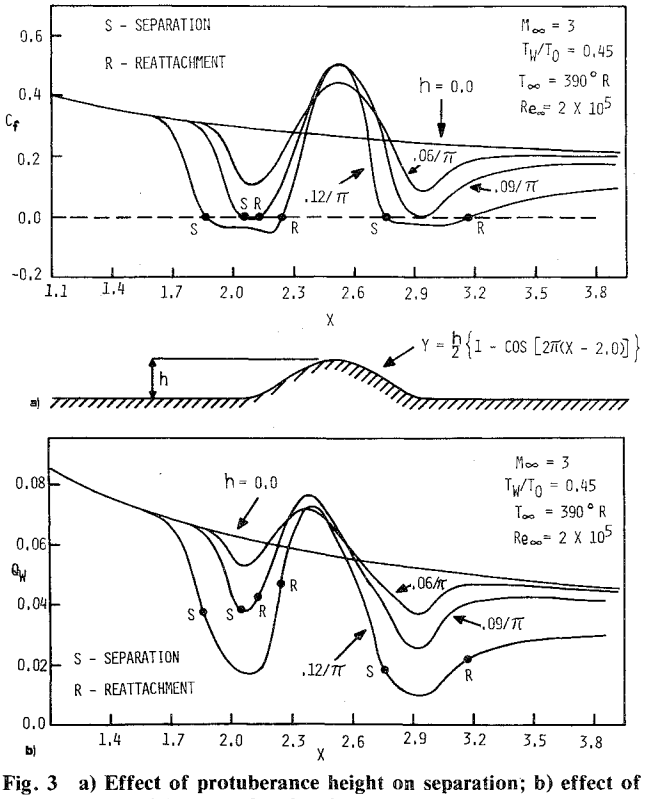

Fig. 3 a) Effect of protuberance height on separation; b) effect of protuberance height on surface heating.

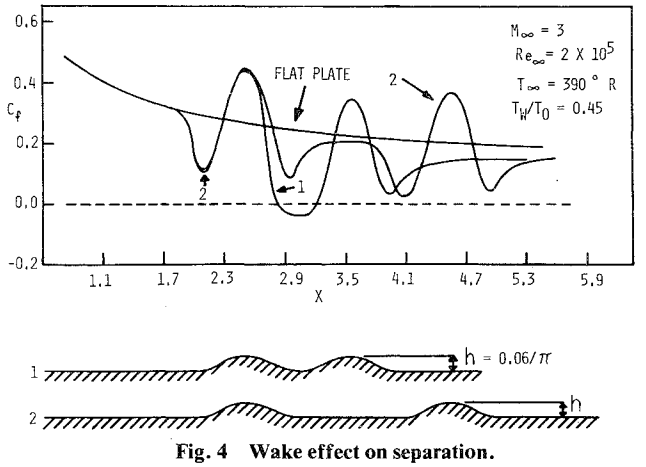

Fig. 4 Wake effect on separation.

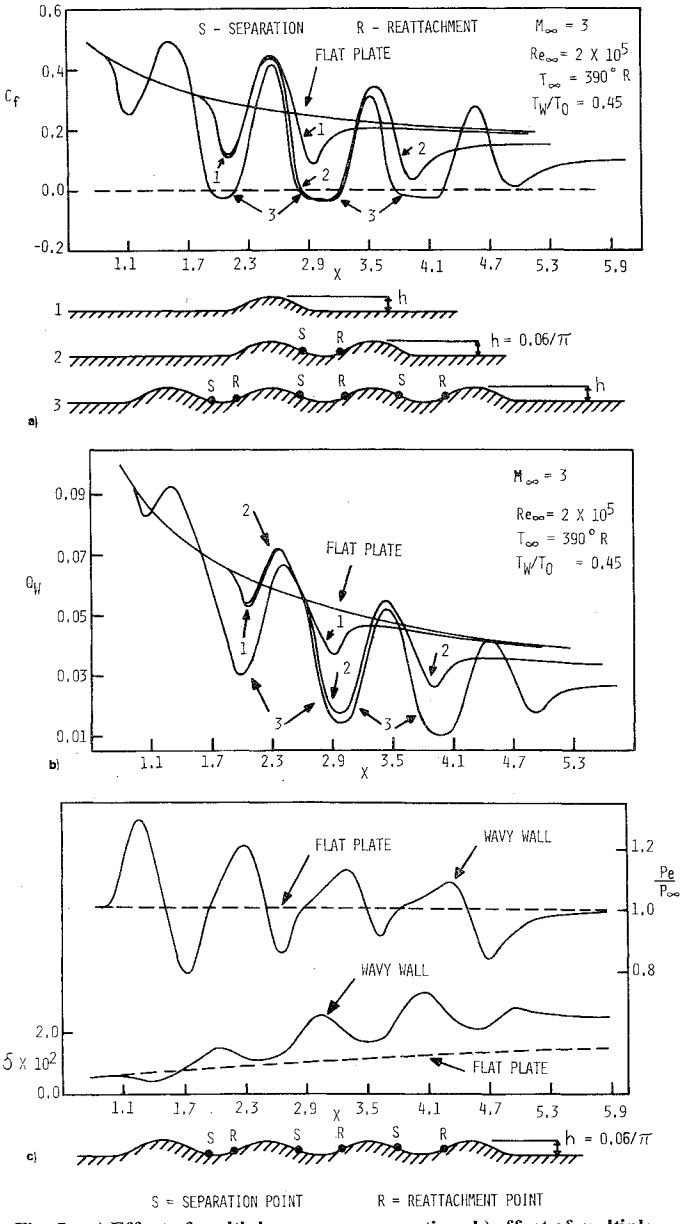

Fig. 5 a) Effect of multiple waves on separation; b) effect of multiple waves on surface heating; c) distribution of pressure and displacement thickness along a wavy wall.

thickness grows as the displacement thickness over the flat plate. However, after separation has occurred (as observed from the C_f distributions of Fig. 5a), both the surface pressure and the displacement thickness are significantly distorted. The pressure develops a plateau-like region in the streamwise direction and the displacement thickness grows in average considerably faster than for the corresponding flat plate case.

Results of a parametric study to identify the influence of the Mach number and Reynolds number on separation characteristics of a single protuberance are shown in Fig. 6a,b. The ratio of the local skin friction to the corresponding flat plate value at the same location and same flow conditions, C_f/C_{fp}, and similarly the heat transfer ratio Q_w/Q_{fp} are compared at two different Mach numbers ($M_\infty = 3$ and 6) and at two Reynolds numbers ($Re_\infty = 1\times10^5$ and 2×10^5). These results show that an increase in the Mach number delays separation, while an increase in Reynolds number has an opposite effect (Fig. 6a,b), these trends being similar to those found in many previous studies of ramp and shock induced laminar separation.

From a practical standpoint, one of the most important points of concern is the maximum heating rate which occurs in the neighborhood of the crest of each protuberance. As shown in Fig. 5b, for a train of waves these heating maxima decrease in the streamwise direction and it would seem that the peak heating at the first wave is of most interest. Figure 7a shows the maximum heating rates over a single protuberance as a function of protuberance height and location. The results of the present calculations indicate that while the boundary-layer remains attached, the relative maximum heating rate increases almost linearly with protuberance height. The same trend was observed for attached turbulent flows over a single protuberance.[12] The solid lines in Fig. 6a representing the semi-empirical predictions developed by Savage and Nagel[13] (shallow wave results) are applicable to attached laminar flow over a sine-wave protuberance. Their semi-empirical formula is

$$\frac{Q_{\max}}{Q_{fp}} = 1 + \frac{1}{2}\{-K_1 + [K_1^2 + 4K_2]^{1/2}\} \tag{14}$$

where, for $M_\infty = 3$ and $T_w/T_0 = 0.45$ the value of K_1 and K_2 are

$$K_1 = 2.895 + K_{21}(1 - h/\delta_{fp})$$
$$K_2 = 2.895 K_{21}(h/\delta_{fp})$$
$$K_{21} = [0.3 + 0.0616(w/\delta_{fp})]^{-1}$$

Q_{fp} and δ_{fp} represent the corresponding undisturbed flat plate heat transfer rate and displacement thickness at the same x location where the peak heating value $Q_{\max}$ over the protuberance occurs. It is noticed that if $h/\delta_{fp} >> 1$ and $K_{21} << 2.895$, we may approximate $K_1 \simeq 2.895 - K_{21}h/\delta_{fp}$ and get $Q_{\max}/Q_{fp} \simeq K_{21}h/\delta_{fp}$. This is in agreement with the observations made earlier from the present calculated results. This empirical correlation is not supposed to be valid for separated flows, as indeed the present results indicate.

Figure 7a also shows that after separation occurs, the maximum heating rates level-off and even drop as the height of the protuberance increases. [One should take into account the fact that the approximation of Eq. (8) to the Prandtl-Meyer relation is less accurate for steeper waves.] This behavior is reminiscent of flow over a rough surface, although

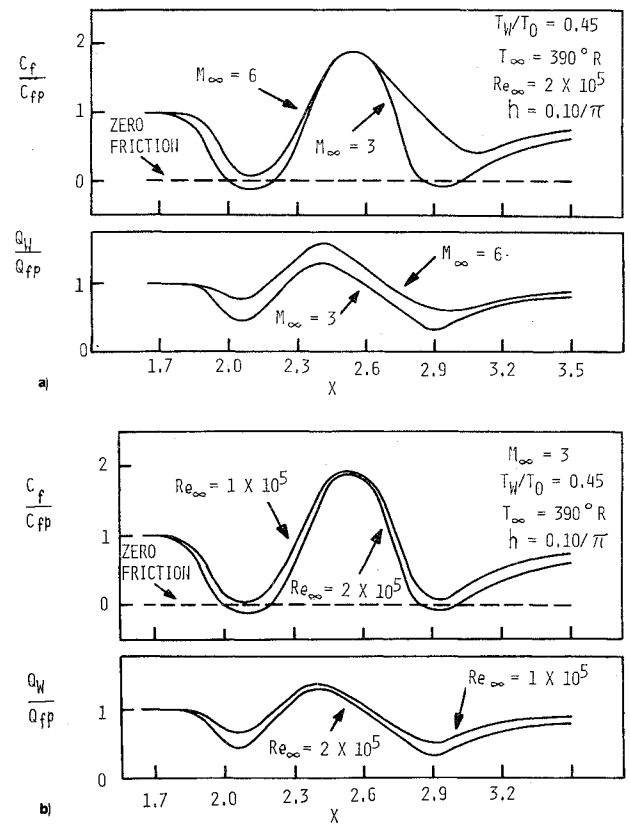

Fig. 6 a) Effect of Mach number on skin friction and surface heating; b) effect of Reynolds number on skin friction and surface heating.

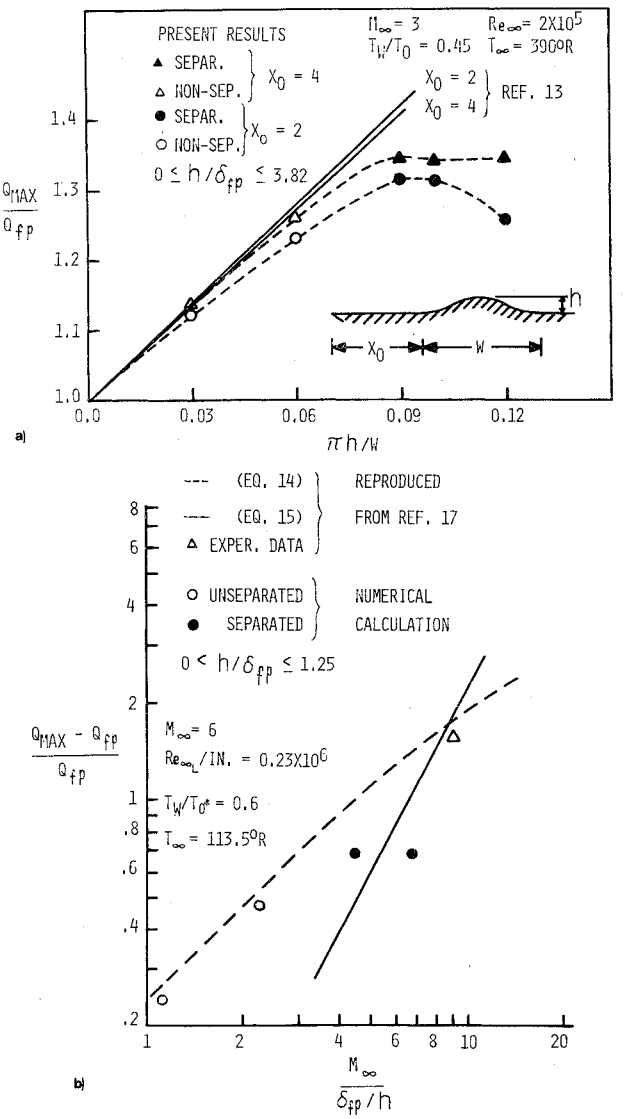

Fig. 7 a) Maximum surface heating on single protuberance; b) correlation of maximum heating over the first sine-wave protuberance.

in details the two flowfields are quite different. In the open literature only one empirical correlation scheme could be found for maximum heating rates over a single sine-wave protuberance (or the first peak for a train of waves) for separated flows given by Bertram et al.[13] as

$$\frac{Q_{\max}}{Q_{fp}} = 1 + \frac{1}{36}\,(M_{e_{fp}}(h/\delta_{fp}))^{1.9} \qquad (15)$$

but, comparisons of the present results at Mach 3 with this relation shows an obvious disagreement.[5] The trend reversal observed in Fig. 7a for large values of h are not predicted by the experimental correlation (Eq. 15). It should be recognized that this empirical correlation relation[14] is based on experimental data for which not all potentially significant parameters were varied. In particular, the experimental data were taken at one value of w/h ($=7.5$) and one value of x_0^* ($=5$ in.). The present calculated separated results were obtained for $x_0=2$ and 4, and $25 \le w/h \le 35$. Some additional experimental data[15,16] also show that this correlation formula is less than satisfactory.

To probe further into this issue, a direct comparison with experimental data[17] was made for laminar flow over a train of sine-waves. The wall profile was given as $y_w^*=h^*\sin[\pi(x^*-5)/0.75]$, (physical distances y_w^*, h^*, and x^* measured in inches). Thus, the junction of the flat plate and the first wave is at $x_0^*=5$ in. The flow conditions were: $M_\infty=6$, $T_w/T_0=0.6$, $T_\infty=113.5°\mathrm{R}$, $\gamma=1.4$, $Re_{\infty_L}/\text{in.}=0.231\times10^6$. The maximum heating was experimentally measured for only $h^*=0$ and 0.1 in. Numerical calculations could not be made at the highest wave height ($h=0.1$; L^* was taken here 1 in.) due to the very sharp corner at the juncture of the first wave and the flat plate. Thus, calculations were performed for the identical conditions and values of $h^*=0$, 0.0125, 0.025, 0.050, and 0.075 in., so that the trend with height h could be identified and hopefully extrapolated to the case of $h=0.1$. For the two largest values of h considered here ($h=0.050$ and 0.075) the flow separated both ahead and behind the first wave peak. For $h=0.0125$, no separation occurred over the first wave and for $h=0.025$, separation occured only ahead of the second protuberance. It was found that the computed maximum heating rate, which occurred on the first peak at $x^*=5.325$ in. in all these cases, leveled off when $h \ge 0.050$, and therefore no substantial change in the computed maximum heating value would be expected at $h=0.10$. Figure 7b shows these results together with the experimental data and the correlation curves reproduced from Ref. 17. According to the numerical results, when the flow was attached on the forward face of the protuberance (where maximum heating occurs) the maximum heating varied linearly with wave height, as predicted by the shallow wave theory Eq. (14). For sake of comparison when plotting the numerical results of $Q_{\max}/Q_{fp}$ in Fig. 7b we use on the abscissa the same value of δ_{fp}^* ($=0.066$ in.) as used in Ref. 17 rather than the presently calculated value ($\delta_{fp}^*=0.060$ in.).

The experimentally measured maximum heating value for the separated case with $h^*=0.1$ in. is very much larger than that expected from the numerical calculations. However, a discrepancy occurs in detailed comparison of the two approaches. It was found that even for the clear flat plate case ($h=0$) the Stanton number results differed; the calculated value was 3.7×10^{-4} while the measured value [see Fig. (10b), Ref. 17] was about 4.5×10^{-4}. This was also noted by Cary et al.[17] who reported that their flat plate laminar heating data was unexplainably higher (by approximately 20%) than that predicted by three different analytical methods.

It is worthwhile noting here a very recent work[18] in which results of an experimental program performed also at NASA's Langley Research Center were reported. The study concerned thick separated turbulent boundary layers over a corrugated flat plate. It was found that the heat transfer was relatively insensitive to the wave height.

It is apparent that more direct comparisons between the present theory and experiments will have to be made before any definite conclusion is made concerning the peak heating rates.

Conclusions

An ADI implicit finite-difference method has been applied to the separated boundary layer interacting with a supersonic outer flow over a wavy wall. Distinct differences in trend of maximum heating rates, growth, and variation of displacement thickness and pressure distribution has been observed for separated flows as compared to attached boundary layers. The numerical results verify a semi-empirical prediction method for peak heating rates for a sine-wave protuberance with attached boundary layer but are not in agreement with an empirical prediction method for separated flow cases. Further comparisons with experimental data would be desirable to resolve this difference. Further, it is recommended that a similar study be carried out for separated turbulent boundary layers.

References

[1] Murphy, J.D., "A Critical Evaluation of Analytic Methods for Predicting Laminar Boundary-Layer Shock-Wave Interaction," *Analytic Methods in Aircraft Aerodynamics,* NASA SP-228, 1970.

[2] Reyhner, T.A. and Flugge-Lotz, I., "The Interaction of a Shock Wave with a Laminar Boundary Layer," Rept. 163, Nov. 1966, Div. of Engineering Mechanics, Stanford University, Stanford, Calif.

[3] Dwoyer, D.L.. "Supersonic and Hypersonic Two Dimensional Laminar Flow Over a Compression Corner," *Proceedings of the AIAA Computational Fluid Dynamics Conference,* Palm Springs, California, July 19-20, 1973, pp. 69-83.

[4] Werle, M.J. and Vatsa, V.N., "New Method for Supersonic Boundary Layer Separations," *AIAA Journal,* Vol. 12, Nov. 1974, pp. 1491-1497.

[5] Polak, A., Werle, M.J., Vatsa, V.N., and Bertke, S.D., "Supersonic Laminar Boundary Layer Flow Past a Wavy Wall with Multiple Separation Regions," Rept. AFL 74-12-15, Feb. 1975, Dept. of Aerospace Engineering, Univ. of Cincinnati, Cincinnati, Ohio.

[6] Werle, M.J., Polak, A., and Bertke, S.D., "Supersonic Boundary-Layer Separations and Reattachment-Finite Difference Solutions," Final Rept. AFL 72-12-1, Jan. 1973, Univ. of Cincinnati, Cincinnati, Ohio.

[7] Mikhailov, V.V., Nieland, V. Ya., and Sychev, V.V., "The Theory of Viscous Hypersonic Flow," *Annual Review of Fluid Mechanics,* Vol. 3, 1971, pp. 371-396.

[8] Werle, M.J., Hankey, W.L., and Dwoyer, D.L., "Initial Conditions for the Hypersonic Shock/Boundary-Layer Interaction Problem," *AIAA Journal,* Vol. 11, April 1973, pp. 525-530.

[9] Garvine, R.W., "Upstream Influence in Viscous Interaction Problems," *The Physics of Fluids,* Vol. 11, July 1968, pp. 1413-23.

[10] Fannelop, T. and Flugge-Lotz, I., "The Laminar Compressible Boundary Layer Along a Wave-Shaped Wall," *Ingenieur-Arciv.* Vol. 33, 1963, pp. 24-35.

[11] Flugge-Lotz, I. and Blottner, F.G., "Computation of the Compressible Laminar Boundary Layer Flow Including Displacement Thickness Interaction Using Finite Difference Methods," TR 131, 1962, Div. of Engineering Mechanics, Stanford University, Stanford, Calif.

[12] Polak, A., "Numerical Study of Supersonic Turbulent Boundary Layer over a Small Protuberance," *AIAA Journal,* Vol. 12, Oct. 1974, pp. 1409-1411.

[13] Jaeck, C.L., "Analysis of Pressure and Heat Transfer Tests on Surface Roughness Elements with Laminar and Turbulent Boundary Layers," NASA CR-537, 1966.

[14] Bertram, M.H., Weinstein, L.M., Cary, A.M., Jr., and Arrington, J.P., "Heat Transfer to Wavy Wall in Hypersonic Flow," *AIAA Journal,* Vol. 5, Oct. 1967, pp. 1760-1767.

[15] Arrington, J.P., "Heat-Transfer and Pressure Distributions Due to Sinusoidal Distortions on a Flat Plate at Mach 20 in Helium," TN D-4907, 1968, NASA.

[16] Weinstein, L.M., "Effects of Two-Dimensional Sinusoidal Waves on Heat Transfer and Pressure Over a Plate at Mach 8.0," TN D-5937, 1970, NASA.

[17] Cary, A.M., Jr. and Morrisette, E.L., "Effect of Two-Dimensional Multiple Sine-Wave Protrusions on the Pressure and Heat-Transfer Distrubutions for a Flat Plate at Mach 6," TN D-4437, 1968, NASA.

[18] Brandon, H.J., Masek, R.V. and Dunavant, J.C., "Aerodynamic Heating to Corrugation Stiffened Structures in Thick Turbulent Boundary Layers," *AIAA Journal,* Vol. 13, Nov. 1975, pp. 1460-1466.